TITLE

An integrated perspective on single-cell and spatial transcriptomic signatures in high-grade gliomas

Authors & affiliations

Célia Lemoine[1], Marc-Antoine Da Veiga[1], Bernard Rogister[1,2], Caroline Piette[1,3†] & Virginie Neirinckx[1*†].

[1] Laboratory of Nervous System Disorders and Therapy, GIGA Institute, University of Liège, 4000 Liège, Belgium

[2] Department of Neurology, CHU of Liège, 4000 Liège, Belgium

[3] Department of Pediatrics, Division of Hematology-Oncology, CHU Liège, 4000 Liège, Belgium

[*]Author to whom correspondence should be addressed.

[†]These authors contributed equally to this work.

Abstract

High-grade gliomas (HGG) are incurable brain malignancies in children and adults. Breakthrough advances in transcriptomic technologies unveiled the intricate diversity of cellular states and their spatial organization within HGGs. We qualitatively integrated 55 neoplastic transcriptomic signatures described in 17 single-cell and spatial RNA sequencing-based studies. Our review delineates a spectrum of cellular states, represented by the expression of specific genes, which can be conceptualized along a "reactive-developmental programs" axis. Additionally, we discussed the potential cues influencing these cellular states, including how spatial organization may impact transcriptomic dynamics. Leveraging these insightful discoveries, we discussed a novel, evolutive way to integrate the different transcriptomic signatures in two or three dimensions, incorporating developmental states, their proliferative capacity, and their possible transition towards reactive states. This integrated analysis illuminates the diverse cellular landscape of HGGs and provides a valuable resource for further elucidation of malignant mechanisms, and for the design of therapeutic endeavors.

Keywords

High-grade gliomas; single-cell RNA sequencing; spatial RNA sequencing; transcriptomic cellular states; spatial organization

Key points

- Malignant transcriptomic states, aligned along an axis ranging from reactive to developmental programs, vary between HGG subtypes.
- Malignant transcriptomic states are plastic, and closely relate to the spatial organization and the evolutive biology of HGGs.

List of abbreviations

AC: Astrocyte cell

DMG: Diffuse midline glioma

G34R/V: Glycine 34 to arginine or valine mutation

GBM: Glioblastoma

H3: Histone 3

HGG: High-grade glioma

IDH: Isocitrate dehydrogenase

K27M: Lysine 27 to methionine mutation

ND: Not determined

NPC: Neural progenitor cell

OC: Oligodendrocyte cell

OPC: Oligodendrocyte progenitor cell

OXPHOS: Oxidative phosphorylation

PRC2: Polycomb repressive complex 2

RG: Radial glial

RNA-seq: RNA sequencing

scRNA-seq: Single-cell RNA sequencing

TAM: Tumor-associated macrophages

TME: Tumor microenvironment

WT: Wildtype

1. Introduction

High-grade gliomas (HGGs) are very aggressive malignancies with poor prognosis, both in adults and children. In 2016 and 2021, the World Health Organization classification considerably evolved, providing a complete histomolecular stratification of adult-type and pediatric-type HGGs, represented in two categories (Fig. 1) [1], [2]. The most aggressive adult-type HGGs are classified as grade 4 *isocitrate dehydrogenase* (*IDH*)-mutant astrocytomas and *IDH*-wildtype (WT) glioblastomas (GBM) [2], the latter being the most common primary brain tumor in adults [3]. Median age at diagnosis is 57 and 68 years respectively. Median survival only reaches 25 months for grade 4 *IDH*-mutant astrocytoma and 10 months for GBM [4], despite standard treatments consisting of maximal surgical resection followed by radiotherapy with concomitant and adjuvant chemotherapy [5]. In comparison, pediatric-type HGGs comprise four molecularly-defined subtypes: diffuse midline glioma (DMG) H3 K27-altered (K27M mutation in histone *H3F3A* or *HIST1H3B* genes); diffuse hemispheric glioma, H3 G34-mutant (G34R/V mutation in *H3F3A gene)*; diffuse pediatric-type HGG, H3-WT and *IDH*-WT; and infant-type hemispheric glioma [2]. Precise epidemiological data are scarce for these recently defined subtypes. In a comprehensive molecular meta-analysis of pediatric-type HGGs, median overall survival of 11 months in DMG H3.3K27M, 15 months in DMG H3.1K27M, 18 months in H3 G34-mutant and 17.2 months in H3-WT and *IDH*-WT were reported [6]. Currently, therapeutic strategies consist of surgical resection, when feasible, followed by radiotherapy with or without the adjunctive use of temozolomide, depending on the molecular subtype [7].

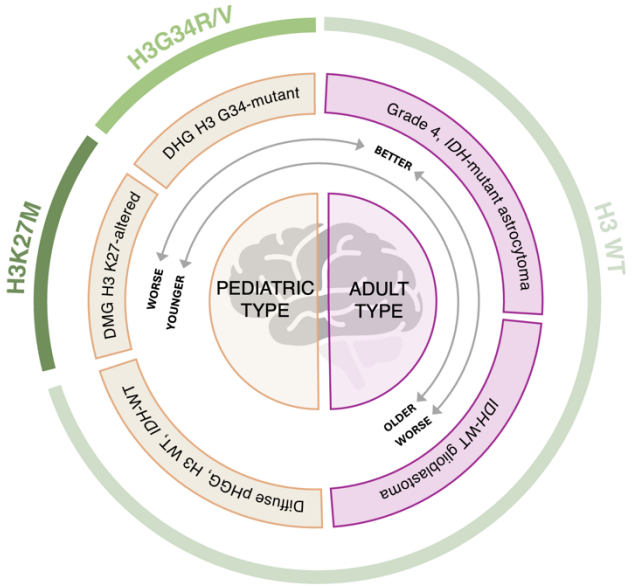

Fig. 1 Schematic view of the three HGG subgroups included in the analysis with their corresponding histo-molecular and epidemiological characteristics. Based on the tumor types included in the 16 selected studies, we distinguished three HGG subgroups: (1) H3K27M and (2) H3G34R/V, both presenting a histone H3 mutation and part of the pediatric-type HGGs in the last WHO CNS5 classification, and (3) H3 wildtype or not determined (H3 WT/ND), potentially including both pediatric- and grade 4 adult-type HGGs. This figure is inspired by the graphical abstract of Mackay et al., 2017.

A characteristic feature of both adult-type and pediatric-type HGGs is the complex heterogeneity, hindering therapies. Tumor heterogeneity roots in the coexistence of neoplastic cells and non-neoplastic cells that constitute the tumor microenvironment (TME) [8]. Variable levels of heterogeneity also characterize neoplastic cells themselves, with regard to genetics, epigenetics [9] and transcriptomics. In this review, we chose to concentrate on transcriptomic studies which particularly evolved this last decade thanks to recent technologies such as RNA sequencing (RNA-seq) [10]. At the inter-patient level, pioneering studies highlighted diverse HGG subtypes, including the most known Verhaak *et al.* “Mesenchymal”, “Classical” and “Proneural” subgroups [10], [11]. Years later, it appeared that these studies were only scratching the surface of the deep HGG complexity, with HGG transcriptomics evolving towards single-cell resolution. Single-cell RNA-seq (scRNA-seq) revealed specific gene expression signatures associated with different cell types, functions and states within one tumor [12]. More recently, spatial transcriptomics further allowed the analysis of RNA content linked to spatial information, emphasizing on specific niches and their peculiar gene expression patterns [13]. These crucial analyses represent a large amount of data and efforts, and together have improved the understanding of the highly heterogeneous nature of HGGs, paving the way to more adapted treatments. However, as separated studies, their practical implementation in HGG diagnosis, management and therapy has yet to be demonstrated.

Convinced about the pivotal role of transcriptomics in HGGs, we aimed to provide a review integrating recent studies addressing the transcriptomic intratumoral neoplastic heterogeneity in HGGs to strengthen individual observations and provide scientists in the neuro-oncology field with a hindsight vision of the recent literature. The numerous transcriptomic-based cellular states of cancerous HGG cells and their associated genes described in single-cell and spatial RNA-seq analyses were qualitatively aligned along a “reactive-developmental programs” axis, providing a clear overview at a single glance. To present a comprehensive picture of highly aggressive malignancies developing in the brain, we compared the molecularly distinct adult-type HGGs, referred to as H3 WT or not determined (H3 WT/ND), with pediatric-type DMG H3 K27-altered (H3K27M) and diffuse hemispheric glioma H3 G34-mutant (H3G34R/V), in order to report similarities and disparities. We also discussed some internal and external cues behind cellular states dynamics, the new insights into HGG spatial organization and the perspectives in clinics. Beside our reviewing work, we proposed a new vision on cellular state evolution.

2. Methods

2.1. Study selection criteria

We selected 17 scRNA-seq and spatial RNA-seq studies addressing HGG heterogeneity, that were published after the Patel *et al.*' 2014 pioneering paper. Each of the chosen papers proposed novel, original gene expression signatures of the neoplastic cells in adult-type and/or pediatric-type HGGs (Table S1). Transcriptomic signatures from the cells of TME were not considered in this review.

2.2. Alignment of gene expression signatures

In most of the selected studies, authors confronted their emerging neoplastic transcriptomic signatures to previously described ones, to highlight similarities or deviations. Based on these explicit correlations, we qualitatively integrated and arranged 51 cellular states across a color panel that spreads over two major "programs" (reactive and developmental) and integrates three main "cell type" categories (mesenchymal, astrocytic and proneural), strongly in line with the Richards [14] and Verhaak [10], [15] classifications, respectively (Fig. 2). To facilitate the reading and parallel to Fig. 2, we applied the same color coding in the main text at the first mention of each signature.

2.3. Comparison of gene lists

We also sought to provide a clear overview of the most representative genes, expressed by the different cellular states. We listed the genes highlighted for each subgroup in the heatmaps from the original articles (Fig. 2). In addition, we collected the complete lists of genes associated with the different signatures described respectively for H3 WT/ND tumors and for H3K27M tumors, when available (Table S2). These gene lists were compared using the Venn diagram tool of Bioinformatics and Evolutionary Genomics (https://bioinformatics.psb.ugent.be/webtools/Venn/). Based on the three main "cell type" categories (mesenchymal, astrocytic and proneural), genes that were common to at least three lists of the same category and not concurrently present in the mesenchymal and the proneural categories were retained. We further subgrouped the cellular states to best represent the diversity of signatures described in the chosen studies. Mesenchymal signatures were grouped into "hypoxia" and "immune" for H3 WT/ND tumors. Astrocytic signatures remained as a group. Proneural signatures were segregated into "neural progenitor cell (NPC)" and "oligodendrocyte progenitor cell (OPC)" groups for H3 WT/ND tumors, and into "OPC" and "oligodendrocyte cell (OC)" groups for H3K27M tumors. For each gene retained, the percentage of positive lists among those comprised in each subgroup was calculated and displayed in heatmaps (Fig. 3, Table S3 and S4). It must be noted that these gene lists result from different methodological approaches. Different tissue sources and

sampling, sequencing technologies and bioinformatic analyses (Table S1) may finally bring out different gene sets. The aim of the comparison is not to establish new signatures, but to highlight genes that overlap in similar signatures described by different groups beyond technical disparities, as those genes may rightly constitute representative and systematic markers of cellular states.

3. Integrated view of the selected HGG gene expression signatures

Reactive and mesenchymal signatures were identified by several scRNA-seq analyses of HGG tissue, in line with what was previously described at the intertumoral level. These signatures are displayed in the left part of the proposed “reactive-developmental programs” axis (Fig. 2: red panel). In addition, scRNA-seq has unveiled transcriptomic signatures that resemble different stages of the developmental brain. These signatures are depicted in the right side of the axis (Fig. 2: blue panel). In

the following sections, we discuss the similarities among signatures, including the overlap of genes, and the relevance of integrating them in the global perspective of tackling the complex HGG biology.

Fig. 2 Integrated view of HGG signatures based on H3 status and aligned as reactive vs developmental programs. This figure presents an arrangement of transcriptomic signatures derived from recent studies utilizing single-cell RNA-seq and spatial RNA-seq. Following the framework proposed by Richards *et al*. 2021, the figure is divided into two main panels: a red left panel representing reactive programs and a purple/blue right panel for developmental programs. The figure is then categorized based on the histone H3 status: wild-type or not determined (H3 WT/ND) (top), H3K27M mutant (middle), and H3G34R/V mutant (bottom). Genes considered as relevant by the authors (i.e. included in the heatmaps from the original papers) are indicated below their respective signatures. *Also in H3K27M tumors.

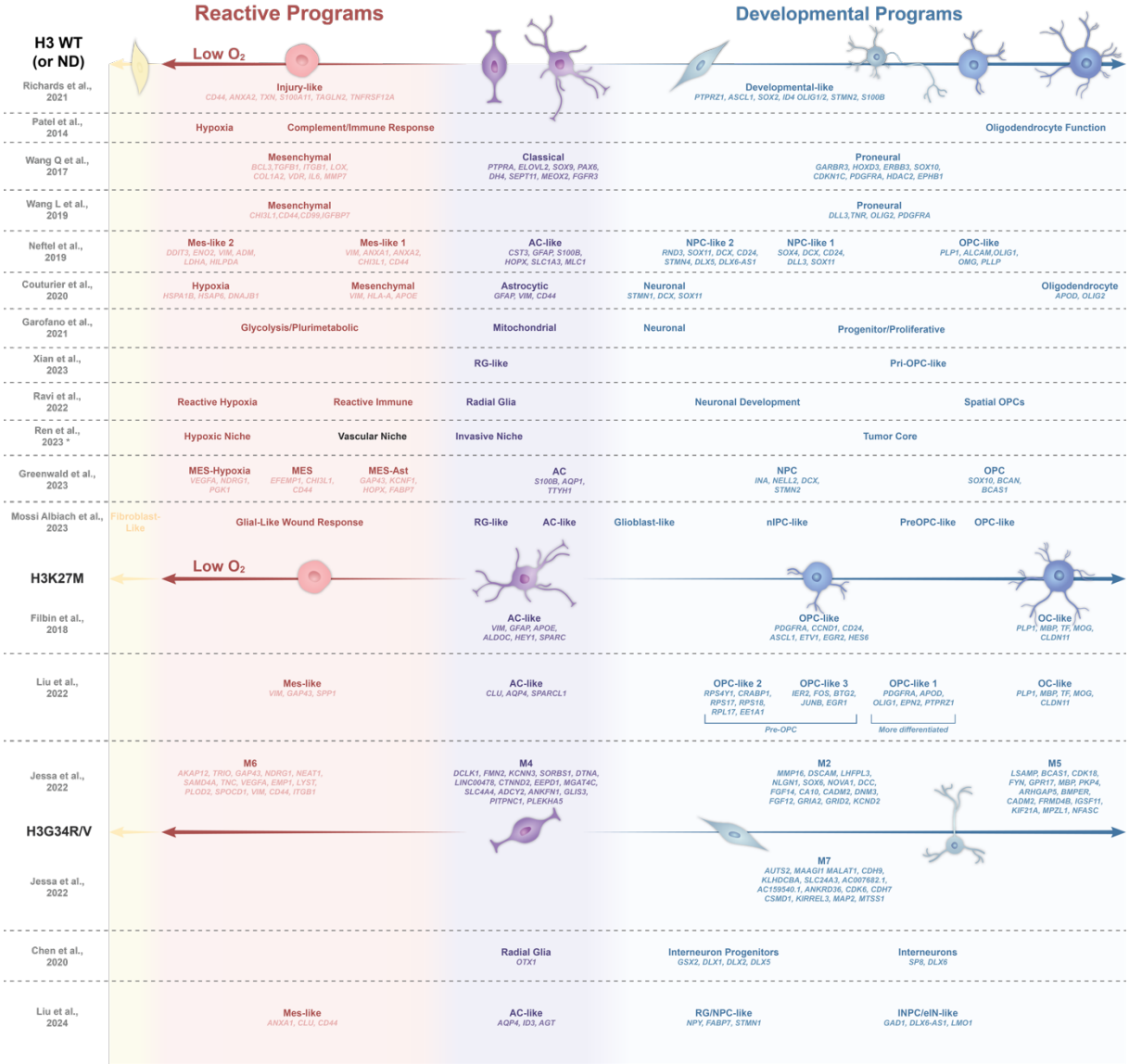

3.1. Reactive Programs – Mesenchymal profile, hypoxia and immune response

In H3 WT/ND HGGs, Wang Q. *et al.* described a single-cell transcriptomic subtype, designated as "Mesenchymal" reminiscent of the bulk classification from Verhaak *et al* [10]. This subtype was associated with *BCL3, TGFB1, ITGB1, LOX, COL1A2, VDR, IL6* and *MMP7* expression [15]. Shortly later,

two studies described a similar axis along which different GBM cellular states were distributed from reactive to developmental programs. The reactive cluster from Wang L. *et al.* was associated with *CD44* and *CHI3L1* expression and is designated as "Mesenchymal", like the previously described subtypes. It overexpressed hypoxia and inflammatory-related genes such as *HIF1a, CSF1, CCL2* and *CXCL2* [16]. Likewise, the "Injury Response" program described by Richards *et al.* was associated with high expression of mesenchymal, inflammatory and immune-related genes such as *CD44, ANXA2, TXN, S100A11, TAGLN2* and *TNFRSF12A* [14].

Other studies distinguished two reactive subgroups. Patel *et al.* described a "Hypoxia" meta-signature and a "Complement/Immune Response" meta-signature [12]. In 2019, Neftel *et al.*, described two mesenchymal meta-modules named "Mes-like 1" and "Mes-like 2", both expressing genes considered as mesenchymal-like, e.g. *VIM*. "Mes-like 2" module was also associated with hypoxia related genes such as *HILPDA* and *ADM*, in addition to stress and glycolysis associated genes such as *DDIT3, ENO2* and *LDHA*. In comparison, "Mes-like 1" signature was hypoxia-independent and was associated with the expression of *ANXA1, ANXA2* and *CD44* [17]. The "Mes-like" subtypes were later correlated with the epithelial-mesenchymal transition, the hypoxic response and the interferon-gamma response, confirming the relationship between reactive states and hypoxia or inflammation [18]. In 2020, Couturier *et al.* also described two groups that could be compared to these reactive programs: the "Hypoxia" group associated with hypoxia responsive genes (*HSPA1B, DNAJB1* and *HSP6A*) and the "Mesenchymal" group associated with high expression of *VIM, HLA-A* and *APOE* [19]. In comparison with these studies that clustered GBM cells based on sole gene expression, Garofano *et al.* provided cancer cell clustering based on pathways. They highlighted a "Glycolytic/Plurimetabolic" signature associated with mesenchymal transformation, immune response and hypoxia, and strongly correlated with other mesenchymal signatures, suggesting a preference for glycolytic pathways in reactive programs. In addition, their signature was correlated with lipids, amino acids, steroids, iron and sulfur metabolism [20].

Recently, spatial transcriptomics provided new insights on the spatial distribution of cells with different gene expression profiles. In line with previous studies, Ravi *et al.* revealed two spatially distinct transcriptomic signatures named "Reactive Hypoxia" and "Reactive Immune" in H3 WT/ND HGGs [13]. Ren *et al.* performed another spatial transcriptomic study in H3K27M DMG and H3 WT/ND HGG patients. They described one main reactive subgroup named "Hypoxic Niche" associated with hypoxia and stress response related genes (Table S2), as well as another spatial signature named "Vascular Niche", associated with vasculogenesis and endothelial cells. This group was more difficult to classify, but partially correlated with the "Reactive Hypoxia" and "Reactive Immune" subgroups from Ravi *et al* [21].

Greenwald *et al.* further segregated the mesenchymal/reactive states into three subgroups: "MES-Hypoxia" associated with a hypoxic signature (*VEGFA, NDRG1* and *PGK1*), "MES" associated with *EFEMP1, CHI3L1* and *CD44* expression and "MES-Ast" (Astrocytic-like Mesenchymal) associated with glioma tumor microtubes related genes (*GAP43, KCNF1* and *PTN*) [22]. Similarly, another study from their research group integrating different scRNA-seq datasets had also suggested several mesenchymal subgroups associated with hypoxia and glycolysis, with astrocytes and immunity and finally, intermediate states, suggesting a strong association between the reactive states and the microenvironment and a possible progression from one reactive state to another [23].

Using enhanced electric single molecule fluorescence *in situ* hybridization, Mossi Albiach *et al.* observed reactive states that correlated with the "Mes-like" signature from Neftel *et al.* Noteworthy, they requestioned the commonly used "mesenchymal" term and rather preferred the term "Glial Wound-Like" that better reflects wound healing activation and hypoxic response in glioma cells [24]. In contrast, they uncovered a rarer "Fibroblast-like" malignant cell subgroup expressing fibroblast markers, e.g. collagens type I (*COL1A1, COL1A2*) and III (*COL3A1, DCN*, and *LUM*), which they considered as a mesenchymal state *per se* [24].

Altogether, reactive programs have been identified in most H3 WT/ND HGG tumors and can be further segregated in response to hypoxia and to inflammation/immune response, with a panel of intermediate states proposed in few studies. Fig. 3 displays the genes associated with the main different programs. For example, hypoxia-responsive and glycolytic genes such as *NDRG1, PGK1, LDHA, ADM, HILPDA* and *VEGFA* are representative genes commonly found in hypoxic signatures whereas genes such as *CD44, FTL, CHI3L1, VIM* and *ANXA2* seem to be associated with reactive signatures in general.

In comparison, reactive programs are rare in pediatric HGGs. In 2018, the pioneering scRNA-seq study from Filbin *et al.* on H3K27M HGGs did not uncover a reactive state [25]. However, few years later, a re-analysis of their dataset highlighted the presence of so-called mesenchymal states. These were mostly associated with an astrocytic and immune signature, rather than to a hypoxic response [23]. In parallel, Liu *et al.* performed scRNA-seq on a wide cohort of both adult and pediatric patients with H3K27M DMGs and unveiled a subset of malignant cells presenting a "Mes-like" signature associated with the expression of *VIM, GAP43* and *SPP1*. This program was enriched in adult patients, compared to young children [26]. Moreover, Jessa *et al.* uncovered a "M6"-coded module, which was partially associated with hypoxia in a large cohort of H3K27M DMGs [27]. Of note, the aforementioned Ren *et al.* "Hypoxic Niche" signature was also highlighted in H3K27M HGGs [21]. Some representative genes are common to H3 WT/ND and H3K27M HGGs, such as *SLC2A3, ADM, PGK1, CD44, VIM* and *SPARCL1* (Fig. 3).

A "Mes-like" program associated with the expression of *ANXA1*, *CLU* and *CD44* was recently described by Liu *et al.* in H3G34R/V HGGs. The proportion of Mes-like cells was described as very

heterogenous across patients, with these cells undetected in some tumors, potentially explaining the discordance between studies [28].

In summary, the reactive cellular states appear more enriched in H3 WT/ND HGGs than in H3K27M and H3G34R/V HGGs and were mostly associated with immune and hypoxic responses, with variations depending on sample types and methods. The diversity of these cellular states, their dependence to multiple external influences as well as their actual origin remain to be untangled.

3.2. Developmental Programs - Astroglial, oligodendroglial and neural-like signatures

Developmental signatures associated with astrocytic, neuronal and oligodendroglial fates were also described in HGGs. They are presented in the middle-to-right part of the "reactive-developmental programs" axis (Fig. 2: purple-to-blue panel), aligned to the "Developmental-like" program proposed by **Richards *et al.***, opposite to the "Injury response" program. The "Developmental-like" program was associated with the expression of genes implicated in neurogenesis and gliogenesis, such as *PTPRZ1, ASCL1* and *SOX2* [14] , also consolidated in the "Proneural" program from **Wang L. *et al.*** expressing *ASCL1* and *OLIG2* [16]. Additional investigations have delineated more detailed developmental signatures associated with astrocytic, neuronal and oligodendroglial fates.

Astrocytes, oligodendrocytes and neurons are the major cell types that are mostly generated during the embryonic brain development. They arise from specialized, quiescent neural stem cells named radial glial (RG) cells that divide to generate lineage-restricted progenitors, including NPCs and OPCs, which evolve through different differentiation steps to finally give rise to mature neurons and glial cells [29].

3.2.1. Astrocytic and radial glia signatures

In H3 WT/ND HGGs, **Neftel *et al.*** identified a subgroup named "Astrocyte Cell (AC)-like" expressing astrocytic markers such as *GFAP, S100B* and *MLC1* [17], and **Couturier *et al.*** described an "Astrocytic" group, mostly associated with astro-mesenchymal genes such as *GFAP, VIM* and *CD44* [19]. Interestingly, *VIM* and *CD44* were commonly expressed in reactive signatures (Fig.3), showing that astrocytic-like cells could display some reactive features. Despite small disparities, both subgroups strongly correlated with the "Classical" group previously described by **Wang Q. *et al.*** associated with high expression of *PTPRA, ELOVL2, SOX9, PAX6, DH4, SEPT11, MEOX2* and *FGFR3* [15]. Based on spatial transcriptomics, **Mossi Albiach *et al.*** and **Greenwald *et al.*** also described "AC-like" subgroups reminiscent of the Neftel *et al.*' signature, and respectively associated with the expression of *CLU, AQP4, ITM2C, S100B*, *CRYAB* [24] and *S100B, AQP1*, *TTYH1* [22].

Moreover, the pathway-based single-cell study proposed by Garofano *et al.* highlighted a cellular group associated with "Mitochondrial" functions, e.g. oxidative phosphorylation (OXPHOS). This group showed a preferential correlation with the Neftel "AC-like" state, suggesting that OXPHOS programs, while not restricted to one cellular state, are enriched in astrocytic signatures [20]. In another pathway-oriented study, OXPHOS was surprisingly inversely correlated with the "AC-like" state, then requestioning this association [18].

"AC-like" cellular states were also described in H3K27M DMGs by Filbin *et al.* and Liu *et al.*, who respectively characterized this state based on *VIM, GFAP, APOE, ALDOC, HEY1, SPARC* and *CLU, AQP4*, and *SPARCL1* gene panels [25], [26]. In their study, Jessa *et al.* introduced a "M4" module that overlapped with the astrocytic signature [27].

In H3 WT/ND HGGs, Xian *et al.* described a "RG-like" cellular state defined by the expression of *VIM* and *SLC1A3* [30] in line with the initial discovery of these RG-like cells transcriptionally resembling RG cells from non-tumoral fetal brains. The presence of these cells, expressing *PTPRZ1* as a main marker confirms the possible reactivation of developmental programs in HGGs [31]. These "RG-like" cells closely relate to astrocytic signatures and share some marker genes with mesenchymal states, explaining their intermediate position in the "reactive-developmental programs" axis (Fig. 2). Mossi Albiach *et al.* also introduced a "RG-like" subgroup associated with the expression of *SOX2, NES* and *VIM* [24].

Spatial transcriptomic studies further supported the presence of these cellular subgroups in HGGs. Ravi *et al.* described a "Spatial RG" subtype associated with the expression of *HOPX* and *PTPRZ1,* which strongly overlapped with "AC-like" states [13]. Ren *et al.* uncovered an "Invasive Niche" correlating with the "Spatial RG" group from Ravi *et al.* in both H3 WT/ND HGGs and H3K27M DMGs. They identified a high proportion of RG-like cells in this niche, suggesting a role of this cellular subtype in tumor invasion [21].

In H3K27M DMGs, the RG subtype was not initially identified. However, Ren *et al.* further discovered the presence of RG-like cells in these tumors with a deeper analysis of the previously established dataset from Filbin *et al.* They identified a cluster associated with a "RG-like" signature and showed its strong correlation with "astrocyte-like" and "mesenchymal-like" signatures [21]. Finally, in H3G34R/V HGGs, Chen *et al.* showed an enrichment of "Radial Glia" programs associated with the expression of *OTX1* [32], while Liu *et al.* described an "AC-like" program associated with the expression of *AQP4, ID3* and *AGT* [28].

All these findings suggest that a subset of HGG cells appear molecularly close to differentiated astrocytes, but also to RG cells, which speak for more "embryonic-like" transcriptomic profiles and related functional aspects, e.g. cell motility/invasion that are of high relevance in a therapeutic perspective.

3.2.2. Neuronal and Oligodendroglial Signatures

In 2014, Patel *et al.* were the first to describe a group associated with "Oligodendrocyte Function" at the single-cell level, without detailing this signature [12]. In 2019, Neftel *et al.* introduced refined signatures associated with OPCs and NPCs in H3 WT/ND HGGs. The "OPC-like" subgroup was associated with the expression of oligodendroglial genes, e.g. *PLP1, ALCAM, OLIG1, OMG* and *PLLP*. The "NPC-like" signatures were further segregated into two subgroups. Both were associated with the expression of NPC markers such as *DCX* and *SOX11,* but the "NPC-like 1" subgroup also included OPC-related genes, while the "NPC-like 2" subgroup was rather linked to neuronal genes, such as *STMN4, DLX5* and *DLX6-AS1* [17]. These signatures correlated with the more general subgroup previously described by Wang Q. *et al.* named "Proneural", represented by the expression of genes such as *GARBR3, HOXD3, ERBB3, SOX10, CDKN1C, PDGFRA, HDAC2* and *EPHB1* [15]. Couturier *et al.* also proposed "Neuronal" and "Oligodendrocyte" signatures closely related to Neftel signatures as well as to the Wang "Proneural" subgroup. Representative genes of these signatures included *STMN1, DCX* and *SOX11* for "Neuronal", and *APOD* and *OLIG2* for "Oligodendrocyte" [19]. Interestingly, the Garofano *et al.* pathway-based single-cell study also proposed corresponding subgroups. The first is the "Neuronal" signature mostly associated with neuron development and axonogenesis, and the second is the "Progenitor/Proliferative" signature associated with cell cycle progression pathways and neural stem/progenitor markers. Again, these two subgroups correlated with the Neftel "NPC-like" and "OPC-like" signatures and with the Wang "Proneural" subgroup [20]. Interestingly, the "Classical" group from Wang Q. *et al.* was also correlated with these signatures, probably reflecting a certain proliferative and stem-like state of this subgroup that may be due to the close relation between astrocytic states and RG-like profiles. More simply, Xian *et al.* described a "Pri-OPC-like" state associated with OPC markers such as *PCDH15* and *PDGFRA* [30].

Ravi *et al.* confirmed the presence of two transcriptomic spatial groups named "Neuronal Development" and "Spatial OPCs", which correlated with Neftel "NPC-like" and "OPC-like" signatures [13]. These subgroups also correlated with the "Tumor Core" niche described by Ren *et al.*, associated with gliogenesis-related genes such as *ALDOC, OLIG2, PDGFRA, ASCL1* and *SOX10*. This last niche was described in both H3 WT/ND and in H3K27M HGGs [21]. Greenwald *et al.* also described "NPC" and "OPC" cellular states associated with *INA, NELL2, DCX, STMN2* and *SOX10, BCAN, BCAS1* respectively [22]. Mossi Albiach *et al.* proposed more specific subgroups designated as "Glioblast-like", "Neural IPC-like", "PreOPC-like" and "OPC-like" states, even suggesting a greater complexity [24].

In contrast to H3 WT/ND HGGs, only oligodendroglial signatures were described in H3K27M DMGs, and these were further separated in "OPC-like" and "OC-like" as firstly described by Filbin *et*

al. "OPC-like" state was associated with the expression of *PDGFRA, CCND1, CD24, ASCL1, ETV1, EGR2* and *HES6,* while "OC-like" state was associated with oligodendrocyte differentiation-related genes such as *PLP1, MBP, TF, CLDN11* and *MOG* [25]. Similarly, Jessa *et al.* described "M2" and "M5" modules that strongly correlated with OPC and oligodendrocyte lineages, respectively [27]. Liu *et al.* also described "OPC-like" and "OC-like" states with the exception that they further subdivided the "OPC-like" group into three subgroups. "OPC-like 1" was associated with a more differentiated OPC state and the expression of genes such as *EPN2*, while "OPC-like 2 and 3" were more associated with pre-OPC state. "OPC-like 2" was associated with ribosomal proteins related genes such as *RPL17* and *RPS18* whereas "OPC-like 3" was more associated with the expression of immediate early response genes such as *JUNB* and *EGR1* [26].

In comparison, H3G34R/V HGGs seem to be composed of distinct cell states, without oligodendroglial signatures, but rather with neuronal signatures. Jessa *et al.* unveiled a "M7" neuronal associated module [27]. Chen *et al.* described populations of cells associated with an "Interneuron progenitor" signature, enriched in genes such as *GSX2, DLX1, DLX2* and *DLX5,* and an "Interneuron" signature associated to *SP8* and *DLX6* [32]. Liu *et al.* also observed two transcriptomic programs correlated to less and more differentiated states of GABAergic interneurons. They described a "RG/NPC-like" state associated with the expression of *NPY, FABP7* and *STMN1,* and a "INPC/eIN-like" state associated with the expression of *GAD1, DLX6-AS1* and *LMO1* [28].

In conclusion, these neurodevelopmental signatures substantially differ between HGG subtypes. H3 WT/ND HGGs contain more NPC and OPC-like cells, while H3K27M DMGs are enriched in oligodendroglial signatures segregated in multiple subgroups going from pre-OPCs-like cells to more differentiated OC-like cells. Some OPC-related genes are common to both tumor types such as *PLP1* and *OLIG1*. In H3 WT/ND HGGs, NPC- and OPC-like signatures share many genes, whereas in H3K27M DMGs, *IGSF11, BMPER, NFASC, EPB41L2* and *ARHGAP5* seem to be specific of OC signatures (Fig.2). In contrast, H3G34R/V HGGs are rather enriched in neuron- and interneuron-like signatures.

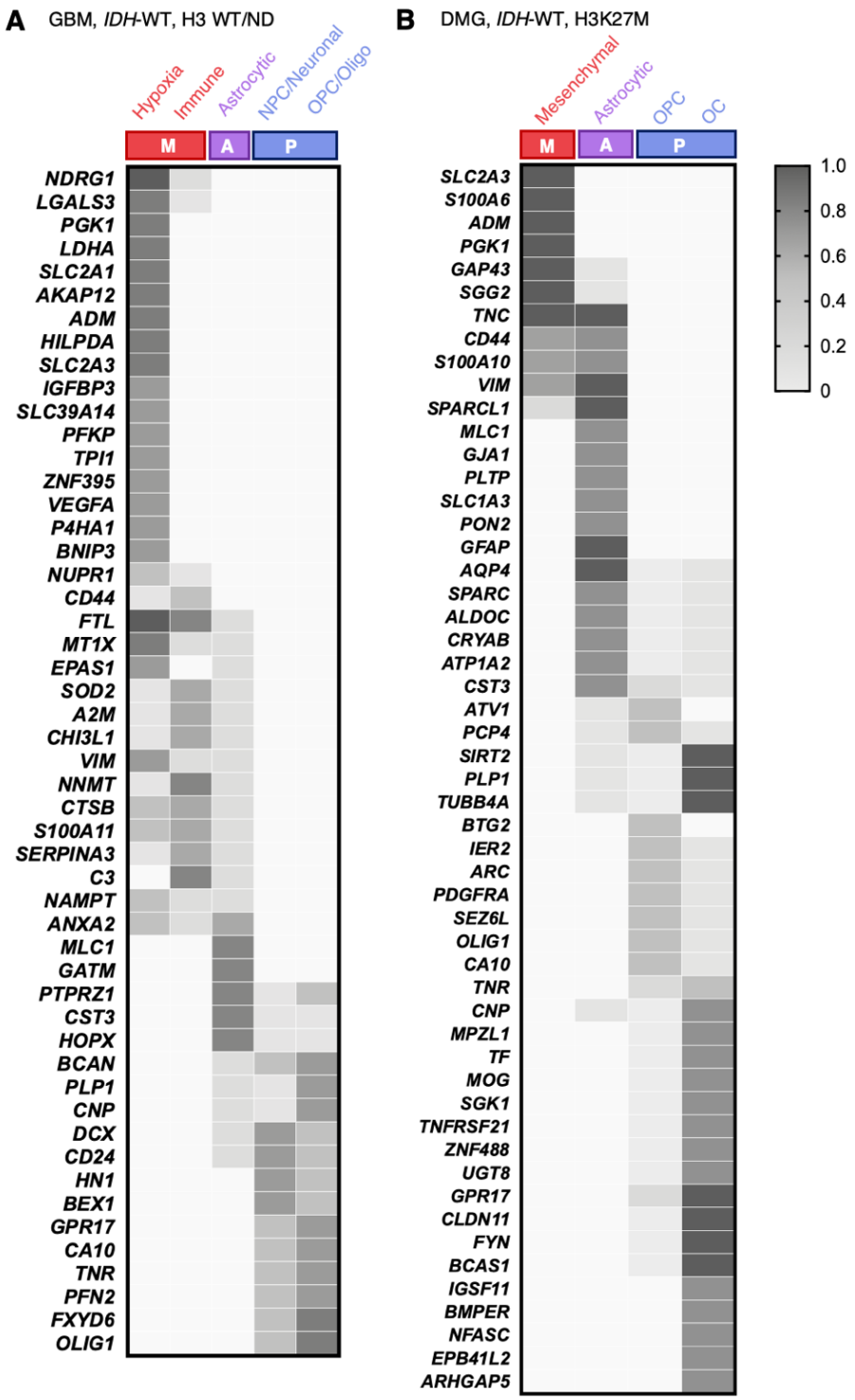

Fig. 3 Heatmap representation of gene overlap across HGG gene expression signatures. Complete gene lists available in 9 RNA-seq studies were analyzed using the Venn diagram tool from Bioinformatics and Evolutionary Genomics. Common genes, excluding mesenchymal and proneural overlaps, were selected. The presence of each retained gene across lists was calculated and depicted in heatmaps. **A.** The heatmap showcases pivotal genes in hypoxia, immune response, astrocytic, NPC/neuronal, and OPC/oligodendrocyte signatures in H3 WT/ND HGGs (=GBMs). **B.** The heatmap displays key genes in mesenchymal, astrocytic, and OPC signatures in H3K27M HGGs (=DMGs). The coverage of a retained gene is depicted from 0 (white) to 100% (gray) in the heatmaps. Abbreviations: M = Mesenchymal family; A = Astrocytic family; and P = Proneural family

3.3. Gene expression signatures associated to the cell cycle

Most scRNA-seq studies also described "Cell Cycle" associated gene expression patterns. Proliferation status is inferred from the expression of numerous genes, forming distinct transcriptomic clusters. Depending on the authors' choice, cell cycle clusters were retained as specific modules or not. Patel *et al.*, Filbin *et al.*, Jessa *et al.* and Liu *et al.* 2024 presented a "Cell Cycle" signature associated with genes such as *TOP2A* and *CDK1* [12], [25], [27], [28]. Greenwald *et al.* also suggested a "Proliferation and Metabolism" subgroup associated with the expression of *TP53, CTNNB1, CNTD1* as well as *SLC16A1, GGCX* and *PHGK1* [22]. Neftel *et al.*, Couturier *et al.* and Liu *et al.* further clustered the cycling cells into two groups, corresponding to "G1/S" phases and the "G2/M" phases [17], [19], [26].

Among tumors, only a small, though varying proportion of cancer cells are cycling. The vast majority of proliferating cells were observed to be progenitor-like cells [17], [19], [21], [22], [24], [25], [33]. This was mainly the case in H3K27M and H3G34R/V HGGs, in which proliferating cells were mainly restricted to OPC-like cells [25], [26] and NPC-like and INPC-like cells [28] respectively. In H3 WT/ND HGGs, cycling cells were found in all cellular states [17]. Interestingly, hypoxia signatures and neuronal niches appeared inversely correlated with cell cycle, suggesting a diminution in proliferating cells in these areas [12], [13], [20].

Based on these observations, it appears that cell cycle related transcriptomic signatures are not mutually exclusive from reactive-developmental signatures. Integrating the cell cycle as a second-dimension axis, as proposed by Wang L. *et al.*, would therefore be more insightful (Fig. 4) [16]. In H3 WT/ND HGGs, in which each major cellular state has the potential to proliferate, it has been suggested to further divide Neftel subtypes into "Non-Proliferating vs Proliferating" Mes-like/AC-like/OPC-like/NPC-like profiles [33], [34], [35]. In comparison, Filbin subtypes in H3K27M DMGs could be distinguished into "Non-Proliferating vs Proliferating" OPC-like states, though this distinction would not apply to AC-like/OC-like/Mes-like cells that were all described as "Non-Proliferating" [34].

4. Intrinsic determinants of HGG cell plasticity

Cellular states are not static but rather highly plastic, especially in H3 WT/ND HGGs [17]. These states are dynamically responsive to multiple intrinsic and extrinsic signals that induce specific state transitions, but also determine the preferential transcriptomic state of a cell within the tumor.

Major genetic alterations correlate with the predominant malignant cell subtype constituting the tumor. In H3 WT/ND HGGs, at the bulk level, "Proneural" tumors were associated with *PDGFRA* alterations, "Classical" tumors with *EGFR* amplification or mutation and *CDKN2A* homozygous deletion and "Mesenchymal" tumors with *NF1* and *PTEN* deletion [10]. At the single-cell level, tumors predominantly "AC-like" were similarly associated with *EGFR* amplification, "OPC-like" with *PDGFRA*

amplification, “NPC-like” with *CDK4* amplification and “Mes-like” with *NF1* mutation [17]. Some genetic alterations were also correlated with the pathway-based cellular signatures, *PTEN, RB1* and *NF1* being often altered in the “Glycolytic/Plurimetabolic” subgroup, *NRAS* and *CDK4* in the “Mitochondrial” subgroup, *ATRX* and *TET1* in the “Neuronal” subgroup and, finally, *PDGFRA* and *EZH2* in the “Progenitor/Proliferative” subgroup [20]. In addition, genetics may influence general spatial organization of the tumor [24].

Epigenetics also influences the cellular plasticity within one tumor [17]. In H3 WT/ND HGGs, cells can harbor different DNA methylation profiles that could be correlated with Neftel “NPC-like” and “OPC-like” signatures, or “AC-like” and “Mes-like” signatures, suggesting that stem-like (NPC/OPC) and differentiated-like (AC/Mes) tumor cells harbor distinct DNA methylation profiles. For example, DNA hypomethylation of polycomb repressive complex 2 (PRC2) targets, linked to the upregulation of these genes, was a hallmark of stem-like state cells, compared to more differentiated cells [36]. It was also shown that DNA methylation diversity was associated with early genetic alterations and cellular states, suggesting that epigenetics likely relates genetics and cellular states [37]. In H3K27M DMGs, the DNA hypomethylation also modulated PRC2 activity downstream gene expression, which may favored the “OPC-like” state enrichment as well as the biased evolution towards “AC-like” state [25].

5. Extrinsic determinants of HGG cell plasticity

5.1. Immune cell interactions

The tumor microenvironment (TME) also plays a crucial role on malignant cellular states. Immune cells represent a considerable percentage of the cells composing the tumor, both in adult-type and pediatric-type HGGs [18], [35], [38], [39], with myeloid cells as the most abundant. Spatial analysis and inferred ligand-receptor interactions have shown that cancer cells are able to interact mostly with these myeloid cells, compared to lymphoid cells [18], [35]. In the brain, the myeloid compartment can be further divided into tumor-associated macrophages (TAMs) derived from microglia, TAMs from blood-derived monocytes, neutrophils, and dendritic cells. The lymphoid compartment encompasses B cells and T cells. The latter are composed of the NK cells, $CD4^+$ and $CD8^+$ T cells. Based on scRNA-seq studies, those immune cell types can be further subdivided into different clusters based on their function which can be more pro-tumorigenic or anti-tumorigenic [35].

Mesenchymal/reactive tumors have been strongly associated with immune cells. Tumor purity analysis demonstrated an increase in TME cells in “Mesenchymal” [15] and in “Glycolytic/Plurimetabolic” H3 WT/ND HGG groups [20], these signatures being associated with high infiltration of neutrophils and macrophages [15], [20]. In spatial transcriptomic studies, reactive niches

showed an increase in tumor-associated myeloid cells and T cells [13]. Furthermore, mesenchymal recurrences from non-mesenchymal newly-diagnosed tumors were associated with an increase in immune cells [15]. It was shown that mesenchymal-like neoplastic cells are more associated with monocyte-derived TAMs with an anti-inflammatory and pro-angiogenic profile in the tumor core, while microglia-derived TAMs with a pro-inflammatory profile are found in the tumor edge and the infiltrating regions [23], [40], [41]. Moreover, mesenchymal-like neoplastic cells were shown to be associated with T cells expressing markers of activation and cytotoxicity [23], [42]. A specific mesenchymal-like profile in TAMs was also observed in the H3 WT/ND tumors with the expression of genes associated with the epithelial-mesenchymal transition and hypoxia [18], [35], [42]. Whether immune cells orient cancer cell states, and/or vice-versa remains to be untangled. It was shown that immune cells were able to induce "Mes-like" signatures *in vivo* and *in vitro,* through the secretion of oncostatin M by TAMs, which then interacts with its receptor on cancer cells [42], [43]. Inflammatory cytokines also drove the expression of injury-like genes in developmental-like glioma cells, *in vitro* [14]. On the other hand, it was shown that mesenchymal-like tumors may have an impact on TAMs which would acquire a mesenchymal-like profile [42], suggesting a crosstalk between neoplastic and non-neoplastic cells shaping the tumor.

It was also observed that the ratio of tumor-associated macrophages (TAMs) derived from monocytes compared to microglia increased in adult vs pediatric patients, suggesting that age-related alterations in the TME may correlate with the diversity of cell types/states among HGGs subtypes [26]. In pediatric HGGs, it was observed that microglia-derived TAMs increase with the mesenchymal-like cancer cell population size, compared to monocyte-derived TAMs [38], suggesting different interactions from the adult-type HGGs.

5.2. Neuron-to-glioma synapses and network integration

HGGs form complex tumors that are deeply integrated in the brain. Glioma cells are influenced by neurons through paracrine signaling and neuron-to-glioma synapses. For example, release of glutamate influences the behavior of glioma cells expressing AMPA receptors, impacting tumor progression and invasion [44], [45], [46], [47], [48], [49]. Both in H3 WT/ND and H3K27M HGGs, synaptic genes were enriched in "OPC-like" signatures and the synapses observed in *in vivo* models resemble synapses formed with normal OPCs [45].

Glioma cells not only physically interact with neurons, but they were also shown to form functional networks with other glioma cells and astrocytes via microtube-associated gap junctions. Those networks strongly support treatment resistance [50], [51]. The integration of glioma cells into networks was shown to be associated with specific transcriptomic states. In *in vivo* models, connected

cells were enriched in the "injury response" signature from Richards *et al*., the "AC-like" and "Mes-like" states from Neftel *et al*. and the "glycolysis/plurimetabolic", "mitochondrial" and "progenitor/proliferative" states from Garofano *et al*. In contrast, unconnected cells were more associated with the "developmental signature" from Richards *et al*., the "OPC-like" and "NPC-like" states from Neftel *et al*. and the "neuronal" state from Garofano *et al*. Those observations were confirmed on human datasets comparing the tumor core and the infiltration regions [46].

Neuron-to-glioma synapses were mostly observed on unconnected cells, increasing their invasive capacities. Those unconnected cells were associated with neuronal and OPC-like states, confirming neuron interactions with those cell states [45], [46]. Here again, these data show how cancer cell states, their functional behavior and the cellular interactions they are engaged in, are intermingled. It is yet to be known how and to what extent network integration and synaptic connections influence malignant cell transcriptomic states, and the other way around.

6. Recent insights in GBM organization and dynamic evolution

Thanks to basic histological techniques, it has been observed for years that HGGs harbor a heterogenous spatial organization linked to different TME features. Following the transcriptomic breakthroughs, there was a desire to better link fundamental observations to new cellular state concepts. In adult-type GBM, this led to the creation of the Ivy Glioblastoma Atlas project. Five distinct classical histological regions, defined as the leading edge, the infiltrating tumor, the cellular tumor, the pseudopalisading cells around necrosis and the microvascular proliferation, were microdissected from GBM biopsies and analyzed for genetic alterations and gene expression profiles. This project highlighted a strong link between classical anatomic features and transcriptomic profiles, which tended to be similar in corresponding histological features [52]. The Ivy Glioblastoma Atlas project is the precursor to spatial transcriptomics, allowing for transcriptomic analysis at the resolution of a few cells.

While the spatial organization of pediatric-type HGGs has yet to be better elucidated, recurrent organizational patterns were highlighted by these recent spatial transcriptomics approaches in H3 WT/ND samples. "AC-like" tumor cells were often localized near "OPC-like" and "NPC-like" malignant cells, whereas, "Mes-like" or "Reactive-like" tumor cells tended to cluster together, suggesting that the "reactive-developmental" cell state axis strongly tunes in on tumor spatial organization and environmental cues.

Interestingly, major spatial transcriptomics observations deepen the understanding behind classical histological features. Developmental states were usually located in proximity to blood vessels, while reactive states were further apart, with hypoxia-related reactive states being the most distant[22], [24], enriched in necrotic regions [13]. Based on these observations and spatial coherence

tests, it was shown that the oxygen level strongly influences the spatial organization of tumors [22], [24], [35]. It was suggested that GBM organizes along the core-to-periphery axis. The tumor core was mostly composed of reactive tumor cells, with hypoxia-associated reactive cells located in the most hypoxic zones, and hypoxia-independent reactive cells located closer to blood vessels. These reactive cancer cells were associated with immunosuppressive monocyte-derived TAMs. In contrast, the tumor edge was well vascularized and rather included malignant cells with developmental profiles, more enriched in proliferating states, as well as microglia-derived TAMs [22], [24], [53]. Consolidating the differences along the core-to-periphery axis, a comparison between the transcriptomic signatures of the cells from the infiltrating tumor and the tumor core highlighted a decreased hypoxic signature in the infiltrating tumor compared to the tumor core and an enrichment in pro-inflammatory microglia compared to the tumor core which was rather enriched in anti-inflammatory and pro-angiogenic macrophages [40]. Of note, a few cells with developmental states were also shown to be locally associated with blood vessels in the hypoxic tumor core, further confirming a key role of the vasculature in GBM spatial structure [24]. This tumor organization dictated by the distance to blood vessels goes along with the single-cell pathway-based study, which showed how tissue organization orchestrates cellular states/profiles through metabolic regulation. The “Mitochondrial” signature associated with OXPHOS correlated mostly with “AC-like” but also “OPC-like” and “NPC-like” cells located close to oxygen supply, while the “Glycolysis/Plurimetabolic” group was associated with “Mes-like” cells distant from blood vessels [20]. Additionnally, spatially resolved metabolomics highlighted an enrichment in glycolysis pathways in “Reactive Hypoxia” cellular state located in necrotic zone compared to an enrichment in pentose phosphate pathways in the developmental states [13].

Based on these spatial organization aspects, a dynamic evolution model of GBM was elaborated. It was suggested that developmental cell states, located at the highly oxygenated tumor edge, proliferate and participate to tumor expansion. As the tumor grows, oxygen levels drop down, which induces leaky blood vessels formation and triggers a chronic wound healing response in cancer cells that switch from developmental to reactive states, related to gradual hypoxia. In the hypoxic TME, recruited monocytes acquire a specific immunosuppressive TAM phenotype and participate to this reactive switch in malignant cells, that then reciprocally modulate TAM profile [24]. Supporting the dynamic evolution model, it was also suggested that developmental cellular state-based tumor growth induces hypoxia which leads to a metabolic switch in tumor cells towards glycolysis activating different adaptative responses such as invasion towards oxygenated regions [13].

Notably, various subtypes of reactive states aligned with distinct developmental stages, indicating the potential transition from different developmental states into corresponding reactive states [24]. This intriguing perspective revises the two branches of the “reactive-developmental” axis into two interdepending dimensions (Fig. 4). This adjustment would better capture the plausible

dynamic transitioning from developmental states to reactive states, in response to the multiple intrinsic and external influences from the TME cells and tissue niches. To what extent such a transition model is relevant to pediatric-type HGGs, in which reactive states have been scarcely described, remains to be discussed.

7. Clinical significance of HGG heterogeneity and transcriptomic states

Given the abundance of data accumulated in the past decade, it is crucial to consolidate the findings and grasp their clinical relevance. A thorough comprehension and integration of diverse transcriptomic and spatial signatures, as proposed in this review, is essential in this perspective. It is also crucial to understand how these signatures may be impacted by standard or new treatments, in order to effectively supplement and/or enhance these therapeutic approaches.

In GBM, associations between transcriptomic subgroups and prognosis appear limited. A potential trend towards improved survival in the bulk "Proneural" subgroup, although this observation may be due to an enrichment of *IDH*-mutant tumors in this group [10]. Patel *et al.* showed that an increased heterogeneity within proneural tumors correlated with a poorer prognosis. The mitochondrial subtype, as defined by Garofano *et al.*, exhibited a favorable survival outcome [20], whereas mesenchymal tumors were associated with decreased survival [15]. Despite these observations, the understanding of HGG transcriptomic profiles has not yet resulted on a clear modification of prognosis and patient outcome.

The landscape seems considerably more complex. The interactions between the different cellular states and with the TME components likely play an important role in determining tumor outcome. A recent paper highlighted a link between the spatial organization of transcriptomic subgroups and the prognosis. For instance, tumors enriched in AC-like cells clustering together, or tumors enriched in “OPC-like” cells interacting with hypoxia-associated Mes-like cells, were both correlated with a poorer prognosis. Conversely, tumors with an increased proximity of AC-like cells with other subtypes were associated with a decreased risk [54]. TME cells were also demonstrated to play a crucial role, with various transcriptomic clusters of myeloid cells exhibiting distinct prognostic associations. Some microglial clusters correlated with better survival, while some macrophage-related clusters were rather associated with a worse survival [18]. A higher T-cell abundance at recurrence was also associated with a better survival [16].

How transcriptomic signatures translate towards clinical outcome is intricate and integrating (spatial) transcriptomic data into the practice could be challenging and costly. Nonetheless, some

researchers have developed algorithms capable of determining transcriptomic subgroups and their organization on histological slides, offering a promising avenue for enhancing clinical routines with low-cost transcriptomic data integration [54].

Gaining insight into the impact of existing treatments on tumor cells is crucial for optimizing therapeutic strategies. Between the newly-diagnosed GBM tumor and the recurrence, a switch in transcriptional state can occur [15], [53], [55], revealing tumor adaptability to treatment. GBM recurrence was associated with an increase in the abundance of normal oligodendrocytes and Mes-like cells, and a decrease in AC-like cells [53], [55]. Additionally, an increase in monocyte-derived TAMs accompanied by a decrease in microglia was observed [53]. Changes in the abundance of transcriptomic states strongly correlated with histological features, emphasizing connections between tumor cells and the TME [55]. Intrinsic mechanisms also contribute to transcriptomic state switches. Hypermutation induced by temozolomide correlated with an increase in proliferating stem-like cells. *NF1* mutation as well as loss of *EGFR* or *PDGFRA* amplification at recurrence likely foster glioma cell transition to a mesenchymal state. Additionally, some recurrence-specific gene upregulations were highlighted within existing signatures. At recurrence, stem-like tumor cells exhibited a higher expression of neuronal signaling-related genes, in comparison with newly-diagnosed tumors, suggesting more interactions with neurons [55].

About pediatric-type HGGs, recent advances have started leveraging the intratumoral heterogeneity of DMGs, here referred to as H3K27M HGGs. The imipridone molecule ONC201 has demonstrated notable efficacy in H3K27M HGG patients and is considered as the greatest recent breakthrough in the field [56], [57]. A recent study used scRNA-seq to investigate the mechanisms underlying the action of ONC201 in H3K27M HGGs. Beside its caseinolytic peptidase P activating effect and downstream impact on cell metabolism, ONC201 was shown to reduce the amount of cycling cells, impoverish “OPC-like” cells and shift up the number of cells with a differentiated, AC-like state [58] (Filbin *et al.* signatures). These findings not only highlight the therapeutic potential of ONC201 in controlling H3K27M HGGs proliferative behavior, but also provide detailed insights into its influence on cell differentiation at the molecular level.

Altogether, ongoing efforts to better comprehend transcriptomic signatures, their association with prognosis, control over cellular states, and their response to treatments are pivotal for advancing the field towards new frontiers. Noteworthy, the fact that HGG cell states differentially include coexisting proliferative and non-proliferative components calls for a reexamination of current antitumor therapies, that so far mostly target cycling cells irrespective of the glioma subtype.

8. Discussion and conclusion

RNA-seq has revolutionized the understanding of HGG biological complexity, highlighting HGG intertumoral and more recently, intratumoral heterogeneity and its dynamics. Different cellular states defined by specific transcriptomic signatures co-exist within one tumor, suggesting different functionalities and vulnerabilities. Cells can transit between these states, underlying the multifaceted functioning of HGGs. Here, we integrated 55 single-cell and spatial transcriptomic signatures recently described in H3 WT/ND tumors, mainly corresponding to GBM, and in H3-altered pediatric-type gliomas, divided into H3K27M and H3G34R/V tumors. We provided a comprehensive overview of these cell signatures by aligning them according to a "reactive-developmental programs" axis, inspired from Richards *et al.* study and describing the associated key genes. With our approach, we opted for a qualitative comparison of gene expression signatures as they are depicted in the original papers, keeping in mind that a genuine reanalysis of the original data may strengthen this alignment. We listed the genes that relate to these signatures with their degree of overlap, that result in simplified, combined gene sets that may further help streamlining the assessment of HGG intratumoral heterogeneity.

The integrated sketch of these various HGG transcriptomic profiles highlights the similarities and differences among HGG subtypes. H3 WT/ND HGGs are very heterogenous, possibly containing a mixture of reactive-like cells associated with hypoxia or immune activation, and developmental-like cells rather resembling normal CNS cells. In contrast, H3K27M HGGs are more enriched in these developmental states, especially "OPC-like" and "OC-like", with very few reactive states. Finally, H3G34R/V gliomas are more associated with interneuron fate. As H3K27M and H3G34R/V HGG subclassifications were only recently introduced, the incidence of H3-altered tumor types has likely been under-estimated these last years, as they were probably included in the H3 WT/ND studies by default. Currently, very few data for H3G34R/V tumors are available compared to other HGG subtypes, and further investigation could uncover new specific cellular states. Of note, other parameters influence the tumor cell composition such as the patient age, and the tumor location. A full-scale picture of each considered tumor sample is a requisite for the proper interpretation of its composition and profile.

A second dimension of heterogeneity, added to the "reactive-developmental" states, is linked to the cell cycle. Although proliferating signatures are more abundant in "stem-like" developmental cell subtypes, all cellular states are endowed with proliferative potential in GBM, while in H3K27M DMG, only "OPC-like" cells can be proliferative.

This two-dimensional heterogeneity taken together with recent indications on the spatial tumor organization highlighted new hypotheses to explain GBM dynamics and implies that

developmental states may evolve toward reactive parallels in an interdependent dimension. It can therefore be postulated that reactive states may represent a third axis of cellular heterogeneity, interdependent with the first developmental axis (including stem-like and more differentiated neural or glial cells) and the second cell cycle axis (from non-proliferating to proliferating).

In this review, we chose to concentrate on the transcriptomic diversity of neoplastic cells, which already represents a very intricate picture of HGGs. However, HGG heterogeneity is far more complex, beginning in the tumor itself, where cancerous cells coexist with cells from the TME. These non-neoplastic cells also play a crucial role in HGG biology, and it is important to note that several studies have also taken advantage from recent advances in transcriptomic technologies to better elucidate the transcriptomic diversity and functionality of the cells from the TME, enlarging the possibility for clinical translation [59], [60], [61]. It is proven that glioma cells interact with various cell types such as immune cells, neurons or even other glioma cells, possibly influencing their transcriptomic state. Immune cells tend to influence a mesenchymal-like transition, whereas interactions with neurons are more associated with OPC-like or NPC-like states. How exactly the cancer cell states are influenced by the interactions with the TME remains to be further elucidated.

In conclusion, this review proposes an integrated, harmonized and evolutive vision on HGG intratumoral heterogeneity. This integration of 17 recent studies further empowers their individual message and shows how the HGG cell types and states align and can dynamically evolve along three axes representing neurodevelopmental diversity, reactive profiles and cell cycle activity. Better apprehending HGG heterogeneity during tumor progression as well as the impact of current

treatments will forge the path towards adjusted therapeutic modalities and ultimately improve patient outcome.

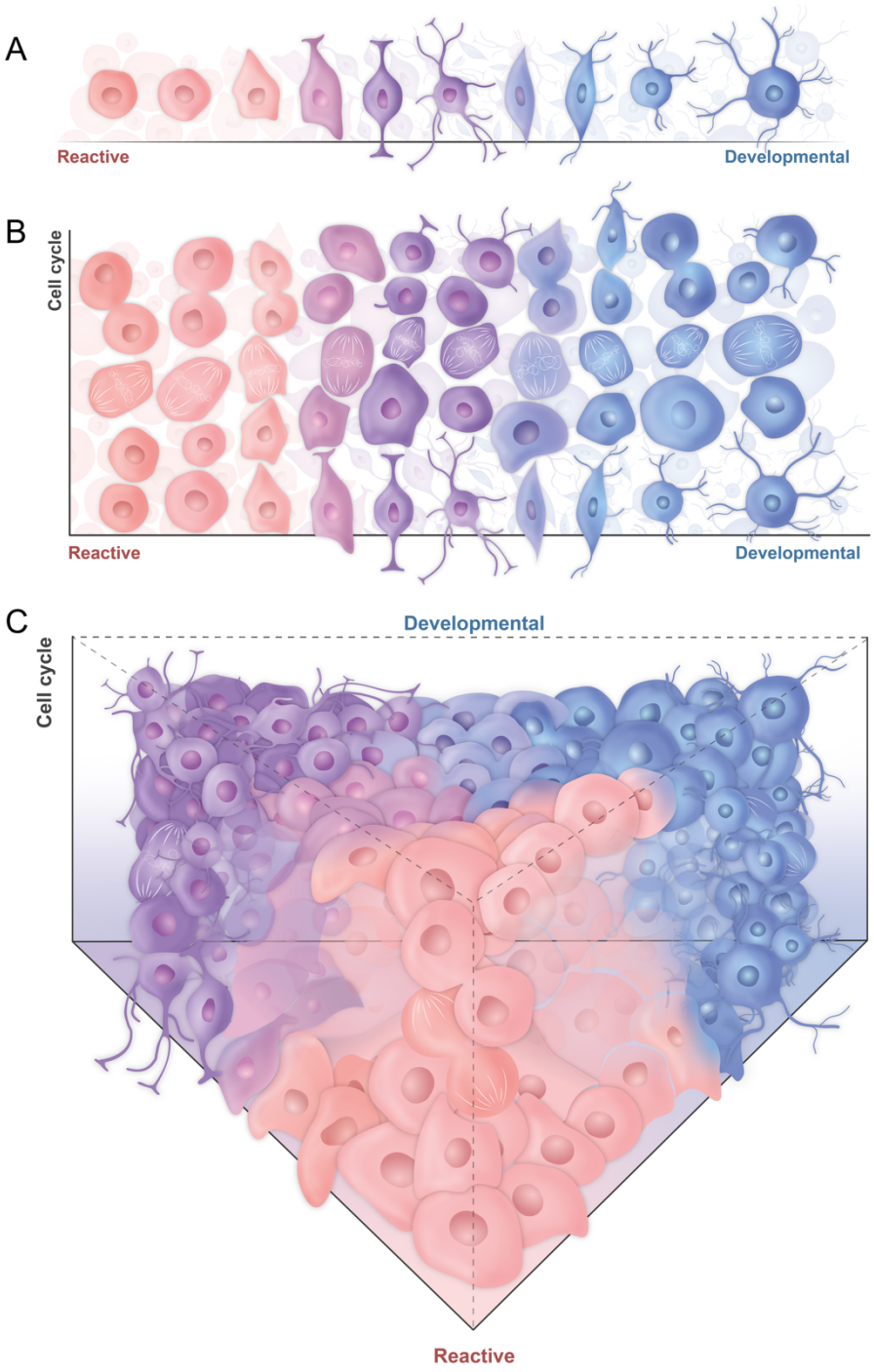

Fig. 4 **Evolutive vision of HGG single-cell and spatial transcriptomic signatures. A.** One-dimension HGG cell state distribution along reactive-developmental programs (based on Richards et al.). **B.** Integration of a cell cycle second dimension to the reactive-developmental HGG cell states (inspired from Wang L. et al). **C.** Tridimensional view on HGG cell states along developmental programs (dimension 1) with different proliferation potential (dimension 2) and capable of evolving towards a reactive state (dimension 3, inspired from Mossi Albiach et al.)

9. Conflict of interest

None declared.

10. Acknowledgements

We thank Louis Baudin (AnimaScience) for scientific illustration.

11. Author contribution

Study design and conceptualization: CL, CP, VN

Manuscript writing: CL, MADV, CP, VN

Analysis: CL

Supervision: CP, VN

Manuscript revision: CL, MADV, BR, CP, VN

12. Funding

The authors are supported by the *Fonds National de la Recherche Scientifique (FNRS)* Belgium (CL), Télévie (MADV) and University of Liège, Belgium.

13. References

[1] D. N. Louis *et al.*, "The 2016 World Health Organization Classification of Tumors of the Central Nervous System: a summary," *Acta Neuropathol. (Berl.)*, vol. 131, no. 6, pp. 803–820, Jun. 2016, doi: 10.1007/s00401-016-1545-1.

[2] D. N. Louis *et al.*, "The 2021 WHO Classification of Tumors of the Central Nervous System: a summary," *Neuro-Oncol.*, vol. 23, no. 8, pp. 1231–1251, Jun. 2021, doi: 10.1093/neuonc/noab106.

[3] Q. T. Ostrom *et al.*, "CBTRUS Statistical Report: Primary Brain and Other Central Nervous System Tumors Diagnosed in the United States in 2016—2020," *Neuro-Oncol.*, vol. 25, no. Supplement_4, pp. iv1–iv99, Oct. 2023, doi: 10.1093/neuonc/noad149.

[4] H. Pinson *et al.*, "Epidemiology and survival of adult-type diffuse glioma in Belgium during the molecular era," *Neuro-Oncol.*, p. noad158, Aug. 2023, doi: 10.1093/neuonc/noad158.

[5] R. Stupp *et al.*, "Radiotherapy plus Concomitant and Adjuvant Temozolomide for Glioblastoma," *N. Engl. J. Med.*, vol. 352, no. 10, pp. 987–996, Mar. 2005, doi: 10.1056/NEJMoa043330.

[6] A. Mackay *et al.*, "Integrated Molecular Meta-Analysis of 1,000 Pediatric High-Grade and Diffuse Intrinsic Pontine Glioma," *Cancer Cell*, vol. 32, no. 4, pp. 520-537.e5, Oct. 2017, doi: 10.1016/j.ccell.2017.08.017.

[7] H. V. Chatwin, J. Cruz Cruz, and A. L. Green, “Pediatric high-grade glioma: moving toward subtype-specific multimodal therapy,” *FEBS J.*, vol. 288, no. 21, pp. 6127–6141, 2021, doi: 10.1111/febs.15739.

[8] P. Sharma, A. Aaroe, J. Liang, and V. K. Puduvalli, “Tumor microenvironment in glioblastoma: Current and emerging concepts,” *Neuro-Oncol. Adv.*, vol. 5, no. 1, p. vdad009, Feb. 2023, doi: 10.1093/noajnl/vdad009.

[9] R. McLendon *et al.*, “Comprehensive genomic characterization defines human glioblastoma genes and core pathways,” *Nature*, vol. 455, no. 7216, pp. 1061–1068, Oct. 2008, doi: 10.1038/nature07385.

[10] R. G. W. Verhaak *et al.*, “An integrated genomic analysis identifies clinically relevant subtypes of glioblastoma characterized by abnormalities in PDGFRA, IDH1, EGFR and NF1,” *Cancer Cell*, vol. 17, no. 1, p. 98, Jan. 2010, doi: 10.1016/j.ccr.2009.12.020.

[11] H. S. Phillips *et al.*, “Molecular subclasses of high-grade glioma predict prognosis, delineate a pattern of disease progression, and resemble stages in neurogenesis,” *Cancer Cell*, vol. 9, no. 3, pp. 157–173, Mar. 2006, doi: 10.1016/j.ccr.2006.02.019.

[12] A. P. Patel *et al.*, “Single-cell RNA-seq highlights intratumoral heterogeneity in primary glioblastoma,” *Science*, vol. 344, no. 6190, pp. 1396–1401, Jun. 2014, doi: 10.1126/science.1254257.

[13] V. M. Ravi *et al.*, “Spatially resolved multi-omics deciphers bidirectional tumor-host interdependence in glioblastoma,” *Cancer Cell*, vol. 40, no. 6, pp. 639-655.e13, Jun. 2022, doi: 10.1016/j.ccell.2022.05.009.

[14] L. M. Richards *et al.*, “Gradient of Developmental and Injury Response transcriptional states defines functional vulnerabilities underpinning glioblastoma heterogeneity,” *Nat. Cancer*, vol. 2, no. 2, pp. 157–173, Jan. 2021, doi: 10.1038/s43018-020-00154-9.

[15] Q. Wang *et al.*, “Tumor evolution of glioma intrinsic gene expression subtype associates with immunological changes in the microenvironment,” *Cancer Cell*, vol. 32, no. 1, pp. 42-56.e6, Jul. 2017, doi: 10.1016/j.ccell.2017.06.003.

[16] L. Wang *et al.*, “The Phenotypes of Proliferating Glioblastoma Cells Reside on a Single Axis of Variation,” *Cancer Discov.*, vol. 9, no. 12, pp. 1708–1719, Dec. 2019, doi: 10.1158/2159-8290.CD-19-0329.

[17] C. Neftel *et al.*, “An integrative model of cellular states, plasticity and genetics for glioblastoma,” *Cell*, vol. 178, no. 4, pp. 835-849.e21, Aug. 2019, doi: 10.1016/j.cell.2019.06.024.

[18] N. Abdelfattah *et al.*, “Single-cell analysis of human glioma and immune cells identifies S100A4 as an immunotherapy target,” *Nat. Commun.*, vol. 13, p. 767, Feb. 2022, doi: 10.1038/s41467-022-28372-y.

[19] C. P. Couturier *et al.*, “Single-cell RNA-seq reveals that glioblastoma recapitulates a normal neurodevelopmental hierarchy,” *Nat. Commun.*, vol. 11, p. 3406, Jul. 2020, doi: 10.1038/s41467-020-17186-5.

[20] L. Garofano *et al.*, “Pathway-based classification of glioblastoma uncovers a mitochondrial subtype with therapeutic vulnerabilities,” *Nat. Cancer*, vol. 2, no. 2, pp. 141–156, Feb. 2021, doi: 10.1038/s43018-020-00159-4.

[21] Y. Ren *et al.*, “Spatial transcriptomics reveals niche-specific enrichment and vulnerabilities of radial glial stem-like cells in malignant gliomas,” *Nat. Commun.*, vol. 14, no. 1, Art. no. 1, Feb. 2023, doi: 10.1038/s41467-023-36707-6.

[22] A. C. Greenwald *et al.*, “Integrative spatial analysis reveals a multi-layered organization of glioblastoma,” *Cell*, p. S0092867424003209, Apr. 2024, doi: 10.1016/j.cell.2024.03.029.

[23] R. Chanoch-Myers, A. Wider, M. L. Suva, and I. Tirosh, “Elucidating the diversity of malignant mesenchymal states in glioblastoma by integrative analysis,” *Genome Med.*, vol. 14, p. 106, Sep. 2022, doi: 10.1186/s13073-022-01109-8.

[24] A. Mossi Albiach *et al.*, “Glioblastoma is spatially organized by neurodevelopmental programs and a glial-like wound healing response,” Cancer Biology, preprint, Sep. 2023. doi: 10.1101/2023.09.01.555882.

[25] M. G. Filbin *et al.*, “Developmental and oncogenic programs in H3K27M gliomas dissected by single-cell RNA-seq,” *Science*, vol. 360, no. 6386, pp. 331–335, Apr. 2018, doi: 10.1126/science.aao4750.

[26] I. Liu *et al.*, “The landscape of tumor cell states and spatial organization in H3-K27M mutant diffuse midline glioma across age and location,” *Nat. Genet.*, vol. 54, no. 12, pp. 1881–1894, 2022, doi: 10.1038/s41588-022-01236-3.

[27] S. Jessa *et al.*, “K27M in canonical and noncanonical H3 variants occurs in distinct oligodendroglial cell lineages in brain midline gliomas,” *Nat. Genet.*, vol. 54, no. 12, pp. 1865–1880, Dec. 2022, doi: 10.1038/s41588-022-01205-w.

[28] I. Liu *et al.*, “GABAergic neuronal lineage development determines clinically actionable targets in diffuse hemispheric glioma, H3G34-mutant,” *Cancer Cell*, vol. 42, no. 9, pp. 1528-1548.e17, Sep. 2024, doi: 10.1016/j.ccell.2024.08.006.

[29] E. Braun *et al.*, “Comprehensive cell atlas of the first-trimester developing human brain,” *Science*, vol. 382, no. 6667, p. eadf1226, Oct. 2023, doi: 10.1126/science.adf1226.

[30] W. Xian *et al.*, “Distinct immune escape and microenvironment between RG-like and pri-OPC-like glioma revealed by single-cell RNA-seq analysis,” *Front. Med.*, Nov. 2023, doi: 10.1007/s11684-023-1017-7.

[31] A. Bhaduri *et al.*, “Outer Radial Glia-Like Cancer Stem Cells Contribute to Heterogeneity of Glioblastoma,” *Cell Stem Cell*, vol. 26, no. 1, pp. 48-63.e6, Jan. 2020, doi: 10.1016/j.stem.2019.11.015.

[32] C. C. L. Chen *et al.*, “Histone H3.3G34-Mutant Interneuron Progenitors Co-opt PDGFRA for Gliomagenesis,” *Cell*, vol. 183, no. 6, pp. 1617-1633.e22, Dec. 2020, doi: 10.1016/j.cell.2020.11.012.

[33] J. J. D. Moffet *et al.*, “Spatial architecture of high-grade glioma reveals tumor heterogeneity within distinct domains,” *Neuro-Oncol. Adv.*, vol. 5, no. 1, p. vdad142, Jan. 2023, doi: 10.1093/noajnl/vdad142.

[34] M. L. Suvà and I. Tirosh, “The Glioma Stem Cell Model in the Era of Single-Cell Genomics,” *Cancer Cell*, vol. 37, no. 5, pp. 630–636, May 2020, doi: 10.1016/j.ccell.2020.04.001.

[35] C. Ruiz-Moreno *et al.*, “Harmonized single-cell landscape, intercellular crosstalk and tumor architecture of glioblastoma,” Aug. 27, 2022, *bioRxiv*. doi: 10.1101/2022.08.27.505439.

[36] R. Chaligne *et al.*, "Epigenetic encoding, heritability and plasticity of glioma transcriptional cell states," *Nat. Genet.*, vol. 53, no. 10, pp. 1469–1479, Oct. 2021, doi: 10.1038/s41588-021-00927-7.

[37] K. C. Johnson *et al.*, "Single-cell multimodal glioma analyses identify epigenetic regulators of cellular plasticity and environmental stress response," *Nat. Genet.*, vol. 53, no. 10, pp. 1456–1468, Oct. 2021, doi: 10.1038/s41588-021-00926-8.

[38] J. DeSisto *et al.*, "Tumor and immune cell types interact to produce heterogeneous phenotypes of pediatric high-grade glioma," *Neuro-Oncol.*, vol. 26, no. 3, pp. 538–552, Nov. 2023, doi: 10.1093/neuonc/noad207.

[39] A. B. Levine *et al.*, "Immuno-oncologic profiling of pediatric brain tumors reveals major clinical significance of the tumor immune microenvironment," *Nat. Commun.*, vol. 15, p. 5790, Jul. 2024, doi: 10.1038/s41467-024-49595-1.

[40] S. Darmanis *et al.*, "Single-Cell RNA-Seq Analysis of Infiltrating Neoplastic Cells at the Migrating Front of Human Glioblastoma," *Cell Rep.*, vol. 21, no. 5, pp. 1399–1410, Oct. 2017, doi: 10.1016/j.celrep.2017.10.030.

[41] M. J. Haley *et al.*, "Hypoxia coordinates the spatial landscape of myeloid cells within glioblastoma to affect survival," *Sci. Adv.*, vol. 10, no. 20, p. eadj3301, doi: 10.1126/sciadv.adj3301.

[42] T. Hara *et al.*, "Interactions between cancer cells and immune cells drive transitions to mesenchymal-like states in glioblastoma," *Cancer Cell*, vol. 39, no. 6, pp. 779-792.e11, Jun. 2021, doi: 10.1016/j.ccell.2021.05.002.

[43] E. Gangoso *et al.*, "Glioblastomas acquire myeloid-affiliated transcriptional programs via epigenetic immunoediting to elicit immune evasion," *Cell*, vol. 184, no. 9, pp. 2454-2470.e26, Apr. 2021, doi: 10.1016/j.cell.2021.03.023.

[44] V. Venkataramani *et al.*, "Glutamatergic synaptic input to glioma cells drives brain tumour progression," *Nature*, vol. 573, no. 7775, pp. 532–538, Sep. 2019, doi: 10.1038/s41586-019-1564-x.

[45] H. S. Venkatesh *et al.*, "Electrical and synaptic integration of glioma into neural circuits," *Nature*, vol. 573, no. 7775, pp. 539–545, Sep. 2019, doi: 10.1038/s41586-019-1563-y.

[46] V. Venkataramani *et al.*, "Glioblastoma hijacks neuronal mechanisms for brain invasion," *Cell*, vol. 185, no. 16, pp. 2899-2917.e31, Aug. 2022, doi: 10.1016/j.cell.2022.06.054.

[47] H. S. Venkatesh *et al.*, "Neuronal Activity Promotes Glioma Growth through Neuroligin-3 Secretion," *Cell*, vol. 161, no. 4, pp. 803–816, May 2015, doi: 10.1016/j.cell.2015.04.012.

[48] H. S. Venkatesh *et al.*, "Targeting neuronal activity-regulated neuroligin-3 dependency in high-grade glioma," *Nature*, vol. 549, no. 7673, pp. 533–537, Sep. 2017, doi: 10.1038/nature24014.

[49] K. R. Taylor *et al.*, "Glioma synapses recruit mechanisms of adaptive plasticity," *Nature*, vol. 623, no. 7986, pp. 366–374, 2023, doi: 10.1038/s41586-023-06678-1.

[50] M. Osswald *et al.*, "Brain tumour cells interconnect to a functional and resistant network," *Nature*, vol. 528, no. 7580, pp. 93–98, Dec. 2015, doi: 10.1038/nature16071.

[51] S. Weil *et al.*, "Tumor microtubes convey resistance to surgical lesions and chemotherapy in gliomas," *Neuro-Oncol.*, vol. 19, no. 10, pp. 1316–1326, Oct. 2017, doi: 10.1093/neuonc/nox070.

[52] R. B. Puchalski *et al.*, "An anatomic transcriptional atlas of human glioblastoma," *Science*, vol. 360, no. 6389, pp. 660–663, May 2018, doi: 10.1126/science.aaf2666.

[53] L. Wang *et al.*, "A single-cell atlas of glioblastoma evolution under therapy reveals cell-intrinsic and cell-extrinsic therapeutic targets," *Nat. Cancer*, vol. 3, no. 12, pp. 1534–1552, 2022, doi: 10.1038/s43018-022-00475-x.

[54] Y. Zheng, F. Carrillo-Perez, M. Pizurica, D. H. Heiland, and O. Gevaert, "Spatial cellular architecture predicts prognosis in glioblastoma," *Nat. Commun.*, vol. 14, no. 1, Art. no. 1, Jul. 2023, doi: 10.1038/s41467-023-39933-0.

[55] F. S. Varn *et al.*, "Glioma progression is shaped by genetic evolution and microenvironment interactions," *Cell*, vol. 185, no. 12, pp. 2184-2199.e16, Jun. 2022, doi: 10.1016/j.cell.2022.04.038.

[56] S. Venneti *et al.*, "Clinical Efficacy of ONC201 in H3K27M-Mutant Diffuse Midline Gliomas Is Driven by Disruption of Integrated Metabolic and Epigenetic Pathways," *Cancer Discov.*, vol. 13, no. 11, pp. 2370–2393, Nov. 2023, doi: 10.1158/2159-8290.CD-23-0131.

[57] E. R. Jackson *et al.*, "ONC201 in Combination with Paxalisib for the Treatment of H3K27-Altered Diffuse Midline Glioma," *Cancer Res.*, vol. 83, no. 14, pp. 2421–2437, Jul. 2023, doi: 10.1158/0008-5472.CAN-23-0186.

[58] J. M. Przystal *et al.*, "Imipridones affect tumor bioenergetics and promote cell lineage differentiation in diffuse midline gliomas," *Neuro-Oncol.*, vol. 24, no. 9, pp. 1438–1451, Feb. 2022, doi: 10.1093/neuonc/noac041.

[59] E. Karimi *et al.*, "Single-cell spatial immune landscapes of primary and metastatic brain tumours," *Nature*, vol. 614, no. 7948, pp. 555–563, 2023, doi: 10.1038/s41586-022-05680-3.

[60] R. R. Maas *et al.*, "The local microenvironment drives activation of neutrophils in human brain tumors," *Cell*, vol. 186, no. 21, pp. 4546-4566.e27, Oct. 2023, doi: 10.1016/j.cell.2023.08.043.

[61] T. E. Miller *et al.*, "Programs, Origins, and Niches of Immunomodulatory Myeloid Cells in Gliomas," Oct. 27, 2023. doi: 10.1101/2023.10.24.563466.

14. Figure Captions

Fig. 1 Schematic view of the three HGG subgroups included in the analysis with their corresponding histo-molecular and epidemiological characteristics. Based on the tumor types included in the 16 selected studies, we distinguished three HGG subgroups: (1) H3K27M and (2) H3G34R/V, both presenting a histone H3 mutation and part of the pediatric-type HGGs in the last WHO CNS5 classification, and (3) H3 wildtype or not determined (H3 WT/ND), potentially including both pediatric- and grade 4 adult-type HGGs. This figure is inspired by the graphical abstract of Mackay et al., 2017.

Fig. 2 Integrated view of HGG signatures based on H3 status and aligned as reactive vs developmental programs. This figure presents an arrangement of transcriptomic signatures derived from recent studies utilizing single-cell RNA-seq and spatial RNA-seq. Following the framework proposed by Richards *et al*. 2021, the figure is divided into two main panels: a red left panel representing reactive programs and a purple/blue right panel for developmental programs. The figure is then categorized based on the histone H3 status: wild-type or not determined (H3 WT/ND) (top), H3K27M mutant (middle), and H3G34R/V mutant (bottom). Genes considered as relevant by the authors (i.e. included in the heatmaps from the original papers) are indicated below their respective signatures. *Also in H3K27M tumors

Fig. 3 Heatmap representation of gene overlap across HGG gene expression signatures. Complete gene lists available in 9 RNA-seq studies were analyzed using the Venn diagram tool from Bioinformatics and Evolutionary Genomics. Common genes, excluding mesenchymal and proneural overlaps, were selected. The presence of each retained gene across lists was calculated and depicted in heatmaps. **A.** The heatmap showcases pivotal genes in hypoxia, immune response, astrocytic, NPC/neuronal, and OPC/oligodendrocyte signatures in H3 WT/ND HGGs (=GBMs). **B.** The heatmap displays key genes in mesenchymal, astrocytic, and OPC signatures in H3K27M HGGs (=DMGs). The coverage of a retained gene is depicted from 0 (white) to 100% (gray) in the heatmaps. Abbreviations: M = Mesenchymal family; A = Astrocytic family; and P = Proneural family

Fig. 4 Evolutive vision of HGG single-cell and spatial transcriptomic signatures. A. One-dimension HGG cell state distribution along reactive-developmental programs (based on Richards et al.). **B.** Integration of a cell cycle second dimension to the reactive-developmental HGG cell states (inspired from Wang L. et al). **C.** Tridimensional view on HGG cell states along developmental programs (dimension 1) with different proliferation potential (dimension 2) and capable of evolving towards a reactive state (dimension 3, inspired from Mossi Albiach et al.)